



# CRISPR-Mediated Activation of $\alpha V$ Integrin Subtypes Promotes Neuronal Differentiation of Neuroblastoma Neuro2a Cells

Sara Riccardi<sup>1,2</sup>, Lorenzo A. Cingolani<sup>1,3\*</sup> and Fanny Jaudon<sup>1,4\*</sup>

<sup>1</sup>Department of Life Sciences, University of Trieste, Trieste, Italy, <sup>2</sup>Department of Experimental Medicine, University of Genoa, Genoa, Italy, <sup>3</sup>Center for Synaptic Neuroscience and Technology (NSYN), Istituto Italiano di Tecnologia (IIT), Genoa, Italy, <sup>4</sup>IRCCS Ospedale Policlinico San Martino, Genoa, Italy

## OPEN ACCESS

### Edited by:

Gabriele Lignani,  
University College London,  
United Kingdom

### Reviewed by:

Gaia Colasante,  
San Raffaele Hospital (IRCCS), Italy  
Mridu Acharya,  
University of Washington,  
United States

### \*Correspondence:

Lorenzo A. Cingolani  
lcingolani@units.it  
Fanny Jaudon  
fjaudon@units.it

### Specialty section:

This article was submitted to  
Genome Engineering and Neurologic  
Disorders,  
a section of the journal  
Frontiers in Genome Editing

Received: 31 December 2021

Accepted: 22 March 2022

Published: 12 April 2022

### Citation:

Riccardi S, Cingolani LA and Jaudon F  
(2022) CRISPR-Mediated Activation of  
 $\alpha V$  Integrin Subtypes Promotes  
Neuronal Differentiation of  
Neuroblastoma Neuro2a Cells.  
Front. Genome Ed. 4:846669.  
doi: 10.3389/fgeed.2022.846669

Neuronal differentiation is a complex process whose dysfunction can lead to brain disorders. The development of new tools to target specific steps in the neuronal differentiation process is of paramount importance for a better understanding of the molecular mechanisms involved, and ultimately for developing effective therapeutic strategies for neurodevelopmental disorders. Through their interactions with extracellular matrix proteins, the cell adhesion molecules of the integrin family play essential roles in the formation of functional neuronal circuits by regulating cell migration, neurite outgrowth, dendritic spine formation and synaptic plasticity. However, how different integrin receptors contribute to the successive phases of neuronal differentiation remains to be elucidated. Here, we implemented a CRISPR activation system to enhance the endogenous expression of specific integrin subunits in an *in vitro* model of neuronal differentiation, the murine neuroblastoma Neuro2a cell line. By combining CRISPR activation with morphological and RT-qPCR analyses, we show that integrins of the  $\alpha V$  family are powerful inducers of neuronal differentiation. Further, we identify a subtype-specific role for  $\alpha V$  integrins in controlling neurite outgrowth. While  $\alpha V\beta 3$  integrin initiates neuronal differentiation of Neuro2a cells under proliferative conditions,  $\alpha V\beta 5$  integrin appears responsible for promoting a complex arborization in cells already committed to differentiation. Interestingly, primary neurons exhibit a complementary expression pattern for  $\beta 3$  and  $\beta 5$  integrin subunits during development. Our findings reveal the existence of a developmental switch between  $\alpha V$  integrin subtypes during differentiation and suggest that a timely controlled modulation of the expression of  $\alpha V$  integrins by CRISPRa provides a means to promote neuronal differentiation.

**Keywords:** integrins, CRISPRa, neurite outgrowth, neuronal differentiation, N2a cells

## INTRODUCTION

Formation of functional neuronal circuits relies on the differentiation of neural stem cells and neural progenitors, a process involving cell cycle arrest and extension of neurites to generate axons and dendrites. Neuronal differentiation is tightly regulated during early brain development and persists, to a certain extent, in the adult nervous system, where it generates new neurons that integrate into

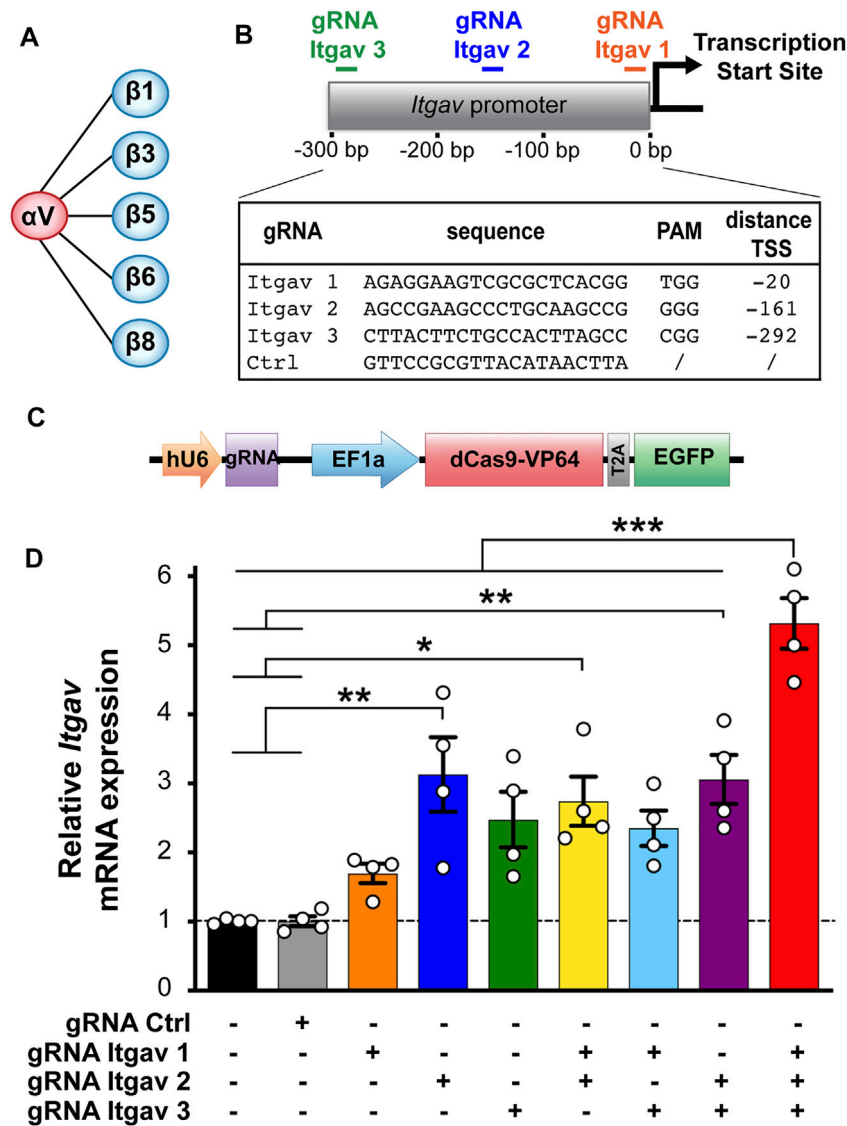


**FIGURE 1** | CRISPRa enhances expression of  $\alpha V$  integrin subunit in N2a cells. **(A)**  $\alpha V$  integrin receptor family. **(B)** gRNA sequences and position of their targets on the *Itgav* promoter. **(C)** Construct used for transfecting murine N2a cells, containing a cassette for expressing the gRNA and one for expressing dCas9-VP64 and EGFP. **(D)** Quantification of  $\alpha V$  integrin mRNA levels in N2a cells 24 h after transfection with the indicated constructs. mRNA expression was normalized to the values of non-transfected samples within the same RT-qPCR plate. \* $p < 0.05$ , \*\* $p < 0.01$ , \*\*\* $p < 0.001$ , one-way ANOVA followed by Tukey's post-test ( $n = 4$  independent experiments).

existing neural networks under physiological conditions or upon injury (Gage and Temple, 2013; Ghosh, 2019; Denoth-Lippuner and Jessberger, 2021).

By transducing chemical and mechanical signals from the extracellular matrix to the intracellular cytoskeleton, the cell adhesion molecules of the integrin family are key regulators of cell migration, neurite outgrowth, synaptogenesis and synaptic plasticity (Cheyuo et al., 2019; Chighizola et al., 2019; Jaudon et al., 2021; Lilja and Ivaska, 2018; Park and Goda, 2016; Prowse et al., 2011; Schmid and Anton, 2003; Thalhammer and Cingolani, 2014; Wojcik-Stanaszek et al., 2011). In mammals, there are 18 alpha and 8 beta subunits, forming 24 integrin

heterodimers (Bachmann et al., 2019; Takada et al., 2007). How different integrin heterodimers cooperate in regulating neuronal differentiation remains, however, largely unknown. The  $\alpha V$  subunit, which is highly expressed in both neural progenitor cells and neurons (Hall et al., 2006; Pinkstaff et al., 1999), dimerizes with five different beta subunits ( $\beta 1$ ,  $\beta 3$ ,  $\beta 5$ ,  $\beta 6$ , and  $\beta 8$ ; **Figure 1A**) to form integrin receptors that recognize an RGD (arginine-glycine-aspartic acid) motif on their extracellular ligands. Previous studies have shown that  $\alpha V\beta 3$  integrin supports the proliferative capacity of neural progenitor cells (Fietz et al., 2010; Stenzel et al., 2014), while  $\alpha V\beta 5$  integrin promotes the differentiation of various types of neurons, such

as cerebellar granule cells (Abe et al., 2018; Oishi et al., 2021) and retinal ganglion cells (Wang et al., 2006), suggesting a role for these integrins in regulating different aspects of neuronal differentiation.

Here, we investigate how enhancing the expression levels of two major  $\alpha$ V integrin subunits ( $\alpha$ V and  $\beta$ 3) regulates neurite outgrowth and branching in an *in vitro* model of neuronal differentiation, the neuroblastoma Neuro2a (N2a) cell line. By combining the CRISPR activation (CRISPRa) technology, which relies on a catalytically inactive nuclease dead Cas9 (dCas9) fused to a transcriptional activator to enhance the expression of genes of interest (Gilbert et al., 2014), with morphological analyses and RT-qPCR, we show that  $\alpha$ V $\beta$ 3 integrin initiates differentiation of N2a cells under proliferative conditions, while  $\alpha$ V $\beta$ 5 integrin likely stabilizes neurites in N2a cells already committed to differentiation. We further show that  $\beta$ 3 and  $\beta$ 5 integrin subunits exhibit a complementary expression pattern during primary neuron development. Our findings reveal that neuronal differentiation requires a finely tuned division of labor between  $\alpha$ V integrin subtypes.

## MATERIALS AND METHODS

### gRNA Design and Plasmid Construction

We used the web tool <http://crispr.mit.edu/> (Ran et al., 2013) to design three gRNAs targeting the region from -10 to -300 bp relative to the transcription start site (TSS) of the mouse *Itgav* gene. As negative control served a non-targeting gRNA sequence (gRNA Ctrl; **Figure 1B**). The gRNA sequences were inserted downstream of the U6 promoter into the pU6-(BbsI)-EF1a-dCas9-VP64-T2A-EGFP plasmid (Jaudon et al., 2019) using the BbsI cloning sites.

### N2a Cell Culture and Transfection

We cultured mouse neuroblastoma N2a cells in Dulbecco's Modified Eagle Medium (DMEM, Gibco) supplemented with 10% FBS, 2 mM glutamine, 100 U/ml penicillin and 0.1 mg/ml streptomycin (complete culture medium), and maintained them in a 5% CO<sub>2</sub> humidified incubator at 37°C. Cells were passaged 2–3 times a week at 80% confluence. For transfection, we seeded N2a cells in 6-well plates in complete culture medium at 200,000 and 100,000 cells/well for RT-qPCR and immunocytochemistry experiments, respectively. Coverslips were coated with 2.5  $\mu$ g/ml poly-D-lysine (PDL; Cat. No. P7405, Sigma) or 5  $\mu$ g/ml fibronectin (Cat. No. F8141, Sigma). The following day, cells were transfected with 4  $\mu$ g DNA/well using the Ca<sup>2+</sup> phosphate method (Thalhammer et al., 2017) and used for experiments 24–72 h post-transfection.

### N2a Cell Differentiation

Twenty-four hours after transfection, complete culture medium was replaced by serum-free medium (formulated as the complete medium but without FBS) to induce differentiation (Schubert et al., 1969). Under these conditions, neurite outgrowth was observed within 12–24 h. Differentiated cells were used for experiments 48 h after serum deprivation.

### Primary Cortical Culture

Cortical neuronal cultures were prepared from P0 C57BL/6J pups as previously described (Korotchenko et al., 2014; Thalhammer et al., 2017), with minor modifications. Briefly, cortices were dissected in ice-cold HBSS, digested with papain (30 U; Cat. No. 3126, Worthington) for 40 min at 37°C, washed and triturated in attachment medium (BME medium supplemented with 10% FBS, 3 mg/ml glucose, 1 mM sodium pyruvate and 10 mM HEPES-NaOH [pH 7.40]) with a flame-polished glass Pasteur pipette. Cells were seeded at a concentration of 95,000 cells/well onto 1.2 cm diameter glass coverslips coated with 2.5  $\mu$ g/ml poly-D-lysine (PDL; P7405, Sigma) and 1  $\mu$ g/ml laminin (L2020, Sigma). After 4 h, the attachment medium was replaced with maintenance medium (Neurobasal medium supplemented with 2.6% B27, 6 mg/ml glucose, 2 mM GlutaMax, 90 U/ml penicillin and 0.09 mg/ml streptomycin). To prevent glia overgrowth, 0.5  $\mu$ M of cytosine  $\beta$ -D-arabinofuranoside (AraC) was added at 1 day *in vitro* (DIV).

### RNA Extraction and RT-qPCR

Total RNA was extracted with QIAzol lysis reagent (Cat. No. 79306, Qiagen) from transfected N2a cells or primary neurons at different developmental stages as previously described (Thalhammer et al., 2018). We prepared cDNAs by reverse transcription of 1  $\mu$ g of RNA using the QuantiTect Reverse Transcription Kit (Cat. No. 205311, Qiagen). RT-qPCR was performed in triplicate with 10 ng of template cDNA using iQTM SYBR<sup>®</sup> Green Supermix (Cat. No. 1708886, Biorad) on a CFX96 Real-Time PCR Detection System (Biorad) with the following universal conditions: 5 min at 95°C, 45 cycles of denaturation at 95°C for 15 s and annealing/extension at 60°C for 45 s. The relative quantification of gene expression was determined using the  $\Delta\Delta$ Ct method. Data were normalized to glyceraldehyde-3-phosphate dehydrogenase (*Gapdh*),  $\beta$ -actin (*Actb*) and hypoxanthine phosphoribosyltransferase 1 (*Hprt1*) by the multiple internal control gene method with GeNorm algorithm (Vandesompele et al., 2002). Sequences of all the primers used are listed in **Supplementary Table S1**.

### Immunocytochemistry

Transfected cells were fixed for 10 min in 4% PFA at room temperature (RT), permeabilized for 10 min at RT with 0.2% Triton-X 100 and blocked for 30 min at RT with 5% NGS. Chicken anti-GFP (1:1,000; Cat. No. AB13970, Abcam) and rabbit anti- $\beta$  tubulin III (1:500; Cat. No. T2200, Sigma-Aldrich) primary antibodies were used for either 2 h at RT or overnight at 4°C. Secondary antibodies were Alexa Fluor488-conjugated anti-chicken (1:1,000; Cat. No. A11039, ThermoFisher scientific) and Alexa Fluor568-conjugated anti-rabbit (1:1,000; Cat. No. A11036, ThermoFisher scientific). We stained cell nuclei with Hoechst (1 mg/ml; Cat. No. B2261, Sigma-Aldrich) and mounted coverslips with ProLong Gold (Cat. No. P10144, ThermoFisher scientific).

### Image Acquisition and Analysis

Three fields of view per coverslip were randomly selected and imaged using a Nikon Eclipse E800 epifluorescence microscope

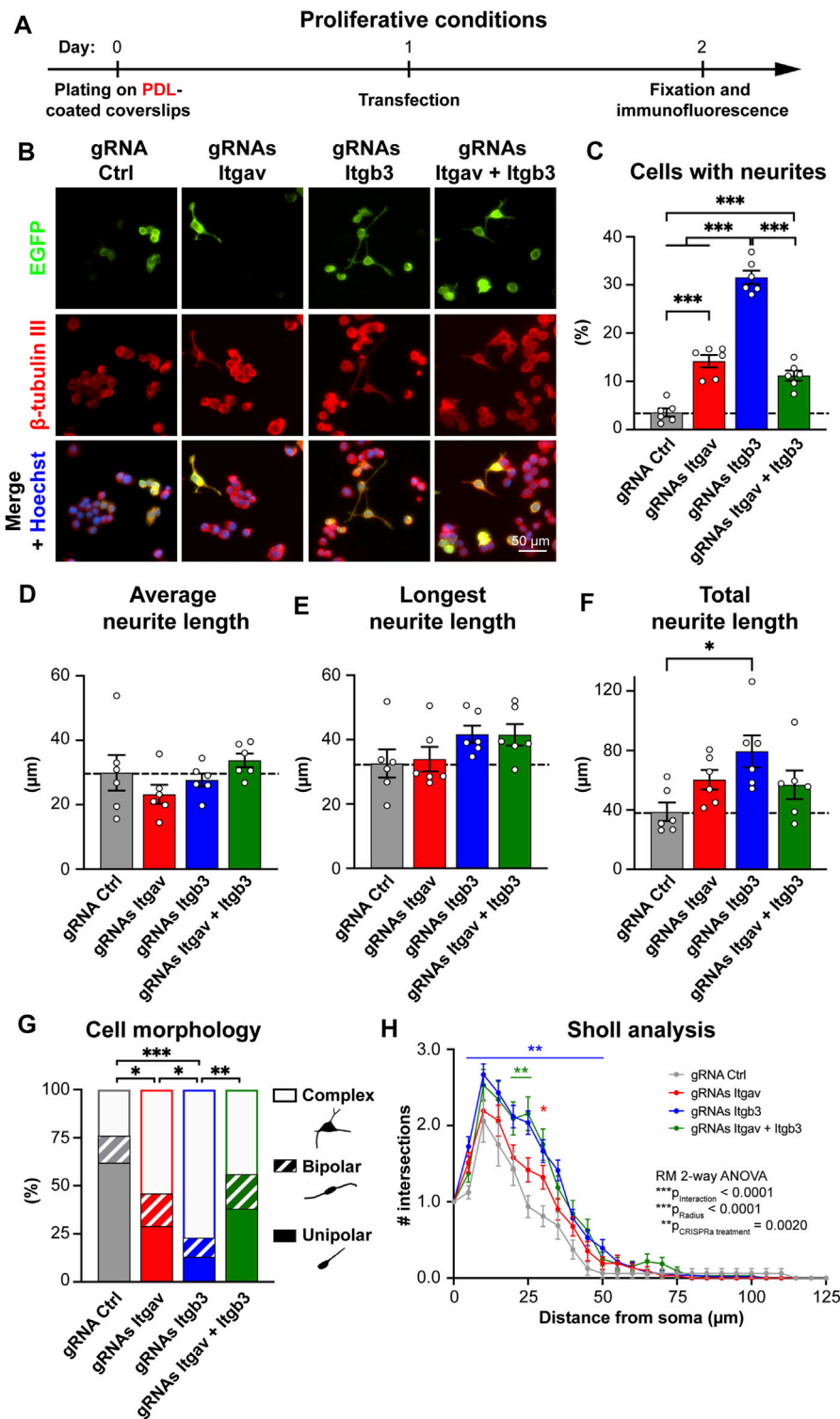


**FIGURE 2 |** CRISPR-mediated activation of *Itgav* and *Itgb3* triggers N2a cell differentiation under proliferative conditions. **(A)** Time course of the experiment. **(B)** Representative images of N2a cells expressing the indicated constructs. Transfection was verified by EGFP expression, β-tubulin III staining was used to trace neurites and Hoechst to stain nuclei. **(C)** Percentage of cells with neurites within EGFP-positive cells for experiments as in **(A,B)**. \*\*\**p* < 0.001, one-way ANOVA followed by Tukey's post-test (*n* = 6 coverslips from four independent experiments). CRISPRa for either *Itgav* or *Itgb3* or both induces differentiation of N2a cells; CRISPRa for *Itgb3* alone is twice as effective as CRISPRa for *Itgav* alone or CRISPRa for *Itgav* and *Itgb3*. **(D–F)** Average **(D)**, longest **(E)** and total neurite length **(F)** of differentiated N2a cells expressing the indicated constructs. \**p* < 0.05, one-way ANOVA followed by Tukey's post-test (*n* = 6 coverslips from four independent cultures). **(G)** Morphological *(Continued)*

**FIGURE 2** | classification of differentiated N2a cells. \* $p < 0.05$ , \*\* $p < 0.01$ , \*\*\* $p < 0.001$ , Chi-square test ( $n = 17, 35, 51$ , and  $34$  cells from four independent experiments for gRNA Ctrl, gRNAs *Itgav*, gRNAs *Itgb3* and gRNAs *Itgav + Itgb3*, respectively). **(H)** Sholl analysis of differentiated N2a cells. \* $p < 0.05$  and \*\* $p < 0.01$  relative to gRNA Ctrl, repeated measures ANOVA followed by Dunnett's post-test ( $n = 17, 35, 51$ , and  $34$  cells from four independent experiments for gRNA Ctrl, gRNAs *Itgav*, gRNAs *Itgb3* and gRNAs *Itgav + Itgb3*, respectively). CRISPRa for *Itgb3* induces a complex arborization.

with a  $\times 20$  objective and a Nikon DXM1200 camera. Neurite length was measured in the red channel ( $\beta$  tubulin III) for all EGFP positive cells using the NeuronJ plugin of ImageJ (<https://imagej.net/NeuronJ>). Cells were considered differentiated if they had one or more processes at least twice as long as their cell bodies. We calculated the percentage of differentiated cells relative to the number of transfected cells (EGFP positive). Sholl analysis was performed on all differentiated transfected cells using the Sholl plugin of ImageJ ([https://imagej.net/Sholl\\_Analysis](https://imagej.net/Sholl_Analysis)) with a starting radius of  $1 \mu\text{m}$  and a radius step size of  $5 \mu\text{m}$ . For morphological analyses, we defined unipolar cells as those with only one unbranched process, bipolar cells as those with two unbranched processes extending in opposite directions from the soma and complex cells as those with more than two unbranched processes or displaying at least one neurite with branches.

## Statistical Analysis

Data are presented as mean  $\pm$  SEM. Statistical significance was set at  $p < 0.05$  and assessed using one-way ANOVA followed by the Tukey's post hoc multiple comparison test, repeated measures two-way ANOVA followed by the Dunnett's post hoc multiple comparison test or two-way ANOVA followed by the Tukey's post hoc multiple comparison test, as specified in figure legends. The Chi-square test was used in **Figures 2G, 3G; Supplementary Figures S1G, S2G** (Prism 7, GraphPad Software, Inc.).

## RESULTS

### CRISPRa Enhances $\alpha\text{V}$ Integrin Expression in N2a Cells

We have explored the possibility of using CRISPRa to enhance transcription of the  $\alpha\text{V}$  integrin subunit as a means to promote neuronal differentiation of the murine neuroblastoma N2a cells. To this end, we have designed three gRNAs targeting the promoter of *Itgav* (the gene encoding  $\alpha\text{V}$  integrin; **Figure 1B**) and expressed them in N2a cells together with dCas9 fused to the transcriptional activator VP64 (Perez-Pinera et al., 2013; Matharu et al., 2019). To minimize experimental variability, we have relied on a single vector designed to co-express a gRNA, dCas9-VP64 and the fluorescent protein EGFP (**Figure 1C**). EGFP allowed us to unambiguously identify transfected cells. As quantified by RT-qPCR 24 h post-transfection, all three gRNAs increased the expression of  $\alpha\text{V}$  integrin by 2 to 3-fold, with gRNA *Itgav-2* being the most effective (**Figure 1D**). We next combined the three gRNAs. While any combination of two of them did not further increase *Itgav* expression, combining all three of them increased it by 5.3-fold (**Figure 1D**). Thus, CRISPRa can be used to boost expression of endogenous  $\alpha\text{V}$  integrin in N2a cells.

### $\alpha\text{V}\beta 3$ Integrin Promotes Neuronal Differentiation of Proliferating N2a Cells

We next addressed whether enhanced  $\alpha\text{V}$  integrin expression promotes neuronal differentiation of N2a cells. When cultured in proliferative conditions (i.e., in medium containing 10% serum; **Figures 2A,B**), only 3.5% of cells expressing gRNA Ctrl exhibited at least one neurite. Maximal CRISPRa for  $\alpha\text{V}$  integrin (using three gRNAs) induced neurite outgrowth in  $\sim 14\%$  of the cells (**Figures 2B,C**). We next compared these effects with those induced by CRISPRa for  $\beta 3$  integrin, a major partner of  $\alpha\text{V}$  integrin in the brain (**Figure 1A**), and whose function has extensively been characterized in neurons in terms of synaptic function (Cingolani et al., 2008; Cingolani and Goda, 2008; McGeachie et al., 2011; McGeachie et al., 2012; Kerrisk et al., 2014; Park and Goda, 2016; Jaudon et al., 2021). To this end, we used two previously characterized gRNAs targeting the mouse promoter of *Itgb3*, the gene for  $\beta 3$  integrin. When used together, these two gRNAs increase  $\beta 3$  integrin expression in N2a cells by  $\sim 6$ -fold (Jaudon et al., 2019); see also **Figure 4A**, top middle panel). Despite a similar efficacy of CRISPRa for the two integrin subunits, activation of *Itgb3* was twice as effective as activation of *Itgav* in inducing neurite outgrowth ( $\sim 32\%$  and  $\sim 14\%$  of differentiated cells for *Itgb3* and *Itgav*, respectively; **Figures 2B,C**). We next co-activated *Itgav* and *Itgb3*. Co-activation was as effective as single gene activation in elevating *Itgb3* and *Itgav* expression (**Figure 4A**, top left and top middle panels), indicating that CRISPRa efficacy is not diluted by targeting two genes (with five constructs) instead of one (with two or three constructs). The effect on neurite outgrowth was nevertheless comparable to that obtained by activating *Itgav* alone ( $\sim 11\%$  and  $\sim 14\%$  of differentiated cells for *Itgb3/Itgav* coactivation and *Itgav* activation, respectively; **Figures 2B,C**), indicating that the effects of  $\alpha\text{V}$  integrin are dominant over those of  $\beta 3$  integrin.

Within the population of differentiated cells, increased expression of *Itgav* or *Itgb3* or both affected neither the average neurite length per cell (**Figure 2D**) nor the length of the longest neurite in each cell (**Figure 2E**). We detected only a significant increase in total neurite length per cell upon *Itgb3* activation (**Figure 2F**). Taken together, these results suggest that  $\beta 3$  integrin, rather than contributing to neurite elongation, promotes a higher number of processes and branches per cell. To verify this hypothesis, we next examined morphology and arborization of the differentiated cells by Sholl analysis. While differentiated cells expressing gRNA Ctrl were mainly unipolar, those transfected with gRNAs targeting *Itgav* or *Itgb3* or both presented predominantly a complex multipolar morphology with branched neurites. The effects were especially prominent when targeting exclusively *Itgb3* (**Figure 2G**). Accordingly, the Sholl analysis revealed that the cells with higher levels of  $\beta 3$  integrin

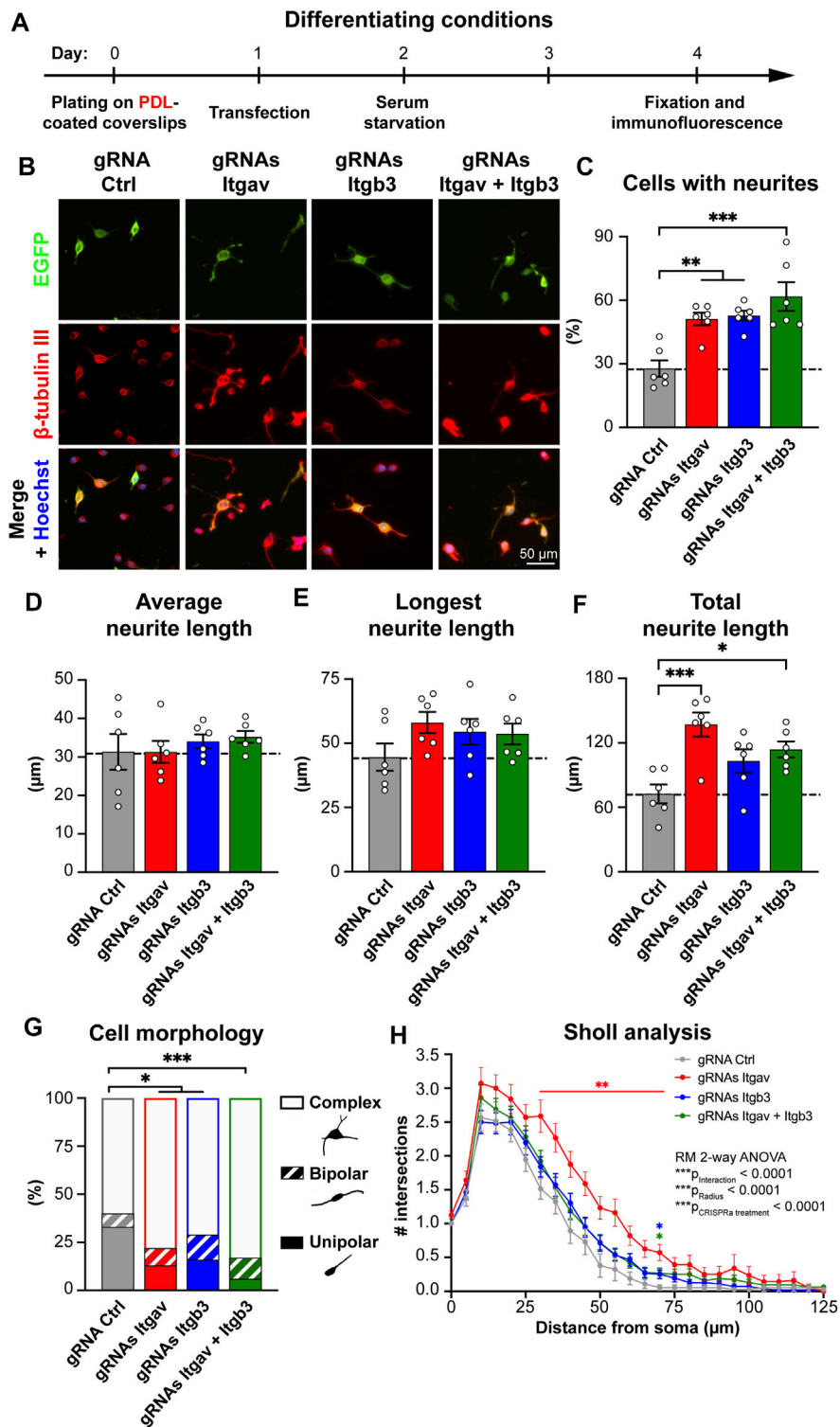


**FIGURE 3 |** CRISPR-mediated activation of *Itgav* supports complex neurite arborization of differentiated N2a cells. **(A)** Time course of the experiment. **(B)** Representative images of N2a cells expressing the indicated constructs. Transfection was verified by EGFP expression, β-tubulin III staining was used to trace neurites and Hoechst to stain nuclei. **(C)** Percentage of cells with neurites within EGFP-positive cells for experiments as in **(A,B)**. \*\* $p < 0.01$ , \*\*\* $p < 0.001$ , one-way ANOVA followed by Tukey’s post-test ( $n = 6$  coverslips from 5 independent experiments). CRISPRa for either *Itgav* or *Itgb3* or both doubles the percentage of differentiated N2a cells, as compared to control conditions. **(D–F)** Average **(D)**, longest **(E)** and total neurite length **(F)** of differentiated N2a cells expressing the indicated constructs. \* $p < 0.05$ , \*\*\* $p < 0.001$ , one-way ANOVA followed by Tukey’s post-test ( $n = 6$  coverslips from 5 independent experiments). **(G)** Morphological classification of (Continued)

**FIGURE 3** | differentiated N2a cells. \* $p < 0.05$ , \*\*\* $p < 0.001$ , Chi-square test ( $n = 55, 82, 75$ , and  $83$  cells from  $5$  independent experiments for gRNA Ctrl, gRNAs *Itgav*, gRNAs *Itgb3* and gRNAs *Itgav + Itgb3*, respectively). **(H)** Sholl analysis of differentiated N2a cells. \* $p < 0.05$ , \*\* $p < 0.01$  relative to gRNA Ctrl, repeated measures ANOVA followed by Dunnett's post-test ( $n = 55, 82, 75$ , and  $83$  cells from  $5$  independent experiments for gRNA Ctrl, gRNAs *Itgav*, gRNAs *Itgb3*, and gRNAs *Itgav + Itgb3*, respectively). CRISPRa for *Itgav* induces a complex arborization.

displayed a more complex arborization than control cells (**Figure 2H**).

Because N2a cells were plated on a polycationic substrate (poly-D-lysine; PDL) that promotes cell adhesion in an integrin-independent manner, some of the differential effects between  $\alpha V$  and  $\beta 3$  integrins on neurite outgrowth might be due to a limited availability of integrin subtype-specific extracellular ligands. To rule out this possibility, we next plated N2a cells on fibronectin, an extracellular matrix protein that binds to all  $\alpha V$ -containing integrins (Johansson et al., 1997). Also under these experimental conditions, activation of *Itgb3* was more effective than that of *Itgav* in inducing neuronal differentiation and promoting a complex arborization (**Supplementary Figure S1**).

Because the  $\beta 3$  subunit pairs exclusively with the  $\alpha V$  subunit in nucleated cells while the  $\alpha V$  subunit pairs with five different beta subunits (**Figure 1A**; Hynes, 2002), these data suggest that *Itgb3* activation skews the composition of  $\alpha V$  heterodimers towards  $\alpha V\beta 3$  integrin, thus promoting effectively neuronal differentiation of N2a cells maintained in proliferative conditions, while *Itgav* activation (alone or in combination with that of *Itgb3*) boosts the expression of  $\alpha V$  heterodimers that restrain  $\alpha V\beta 3$  integrin function under proliferative conditions.

### $\alpha V$ Integrins Promote Neurite Arborization of Differentiated N2a Cells

In response to serum deprivation, N2a cells assume a morphology similar to that of mature neurons (Schubert et al., 1969). We therefore examined how CRISPRa for *Itgav* and *Itgb3* affects differentiation of N2a cells under pro-differentiating conditions (**Figure 3A**). As expected, removal of serum from the culture medium resulted in a higher percentage of differentiated cells in all conditions (**Figures 2B,C** vs. **Figures 3B,C**; for gRNA Ctrl:  $\sim 28\%$  vs.  $\sim 3.5\%$  of differentiated cells, respectively). CRISPRa for either *Itgav* or *Itgb3* or both effectively increased N2a differentiation also under these conditions. As opposed to the proliferative state, the effects of activating *Itgav* were however as robust as those induced by *Itgb3* activation ( $\sim 51\%$  vs.  $\sim 53\%$  of differentiated cells, respectively). Moreover, co-activation of the two genes did not significantly change the percentage of differentiated cells as compared to single gene activation (**Figures 3B,C**;  $62\%$  of differentiated cells), suggesting either a shared mechanism involving up-regulation of  $\alpha V\beta 3$  integrin for the three experimental conditions or a concomitant contribution of different  $\alpha V$  integrin-containing heterodimers to the differentiation process.

We next considered more closely the morphology of the differentiated cells. As in proliferative conditions, changes in the expression levels of *Itgav* or *Itgb3* or both affected neither the average neurite length per cell (**Figure 3D**) nor the length of

the longest neurite in each cell (**Figure 3E**). As opposed to the proliferative conditions, the total neurite length per cell was, however, significantly increased upon *Itgav*, rather than *Itgb3*, activation (**Figure 3F**). Morphological and Sholl analyses further revealed that *Itgav* activation was more, rather than less, effective than *Itgb3* activation in promoting a complex arborization (**Figures 3G,H**). The differences between activation of *Itgav* and *Itgb3* for N2a cell differentiation were even more pronounced when the cells were plated on fibronectin (**Supplementary Figure S2**).

Thus, while  $\alpha V\beta 3$  integrin is extremely effective at inducing neuronal differentiation under proliferative conditions, other  $\alpha V$  integrin-containing heterodimers appear to play a major role in stabilizing a complex arborization at later stages of differentiation.

### Expression of $\alpha V$ Integrin Subunits in N2a Cells and Primary Cortical Neurons

To get insights into which  $\alpha V$  integrin heterodimers may favor branching and stabilization of neurites in N2a cells, we quantified, by RT-qPCR, the mRNA levels of all the beta subunits known to pair with the  $\alpha V$  subunit (**Figure 1A**; Hynes, 2002; Lilja and Ivaska, 2018); under control conditions and following CRISPRa for *Itgav* or *Itgb3* or both (**Figure 4A**). As expected, targeting the promoter of *Itgav* and *Itgb3* with CRISPRa increased the expression level of the respective genes, both in proliferative and differentiating conditions (**Figure 4A**, top left and top middle panels). Strikingly, CRISPRa for *Itgav* increased also the expression of *Itgb5* (the gene for  $\beta 5$  integrin) selectively in differentiating conditions ( $\sim 63\%$  increase relative to control differentiated conditions; **Figure 4A**, bottom left panel). Rather than being due to a direct effect of dCas9-VP64 on the *Itgb5* promoter, the increase in  $\beta 5$  integrin expression levels was likely the consequence of a co-regulation of *Itgav* and *Itgb5*. Indeed, no increase in  $\beta 5$  integrin expression levels was observed under proliferative conditions or under conditions favoring formation of the  $\alpha V\beta 3$  heterodimer (co-activation of *Itgav* and *Itgb3*; **Figure 4A**, bottom left panel).

Taken together, these findings suggest that up-regulation of  $\alpha V\beta 5$  integrin may promote branching and stabilization of neurites at later stages of differentiation in N2a cells.

To address whether the differences between  $\alpha V$  integrin heterodimers are relevant in terms of neuronal differentiation, we next analyzed, in primary cortical neurons, the developmental expression pattern for all the subunits of  $\alpha V$  integrin heteromers. Interestingly, the transcripts for *Itgb3* and *Itgb5* exhibited a complementary expression profile: *Itgb3* peaked at 9 DIV (**Figure 4B**, top middle panel), when dendritogenesis and synaptogenesis reach their maximum rate (Harrill et al., 2015), while *Itgb5* showed a dip during the same time period (**Figure 4B**,

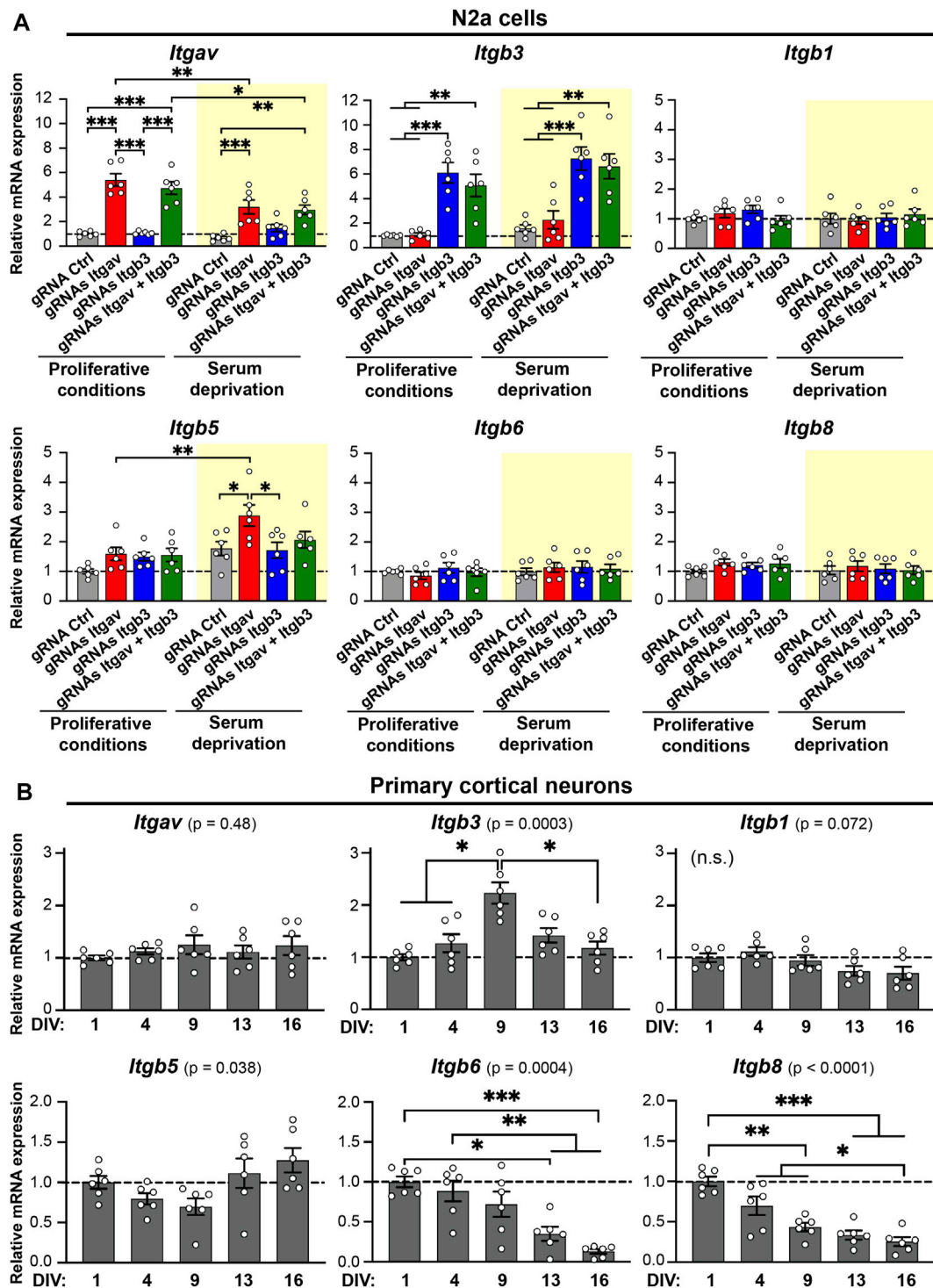


**FIGURE 4** | Expression levels of *Itgav*, *Itgb3*, *Itgb1*, *Itgb5*, *Itgb6*, and *Itgb8* in N2a cells and primary cortical neurons. **(A)** Quantification of *Itgav*, *Itgb3*, *Itgb1*, *Itgb5*, *Itgb6*, and *Itgb8* mRNA levels in response to CRISPRa for *Itgav* and/or *Itgb3* in N2a cells under proliferative conditions (white background) or following serum deprivation (yellow background). mRNA expression was normalized to the values of samples expressing gRNA Ctrl under proliferative conditions within the same RT-qPCR plate. \* $p < 0.05$ , \*\* $p < 0.01$ , \*\*\* $p < 0.001$ , two-way ANOVA followed by Tukey's post-test ( $n = 6$  from 3 independent cultures). CRISPRa for *Itgav* is accompanied by an increase in *Itgb5* expression levels in differentiating N2a cells. F ratio and  $p$  values for two-way ANOVA statistics are as follows, *Itgav*: gRNA effect:  $F_{(3, 40)} = 44.71$ ,  $p < 0.001$  (\*\*\*) ; serum starvation effect:  $F_{(1, 40)} = 13.69$ ,  $p < 0.001$  (\*\*\*) ; Serum starvation  $\times$  gRNA interaction:  $F_{(3, 40)} = 5.351$ ,  $p = 0.003$  (\*\*). *Itgb3*: gRNA effect:  $F_{(3, 40)} = 30.94$ ,  $p < 0.001$  (\*\*\*) ; serum starvation effect:  $F_{(1, 40)} = 5.075$ ,  $p = 0.03$  (\*) ; serum starvation  $\times$  gRNA interaction:  $F_{(3, 40)} = 0.1581$ ,  $p = 0.92$ . *Itgb1*: gRNA effect:  $F_{(3, 40)} = 0.5449$ ,  $p = 0.65$ ; serum starvation effect:  $F_{(1, 40)} = 0.6286$ ,  $p = 0.43$ ; serum starvation  $\times$  gRNA interaction:  $F_{(3, 40)} = 1.189$ ,  $p = 0.33$ . *Itgb5*: gRNA effect:  $F_{(3, 40)} = 4.606$ ,  $p = 0.007$  (\*\*\*) ; serum starvation effect:  $F_{(1, 40)} = 1.189$ ,  $p = 0.33$ . *Itgb6*: gRNA effect:  $F_{(3, 40)} = 1.189$ ,  $p = 0.33$ ; serum starvation effect:  $F_{(1, 40)} = 1.189$ ,  $p = 0.33$ ; serum starvation  $\times$  gRNA interaction:  $F_{(3, 40)} = 1.189$ ,  $p = 0.33$ . *Itgb8*: gRNA effect:  $F_{(3, 40)} = 1.189$ ,  $p = 0.33$ ; serum starvation effect:  $F_{(1, 40)} = 1.189$ ,  $p = 0.33$ ; serum starvation  $\times$  gRNA interaction:  $F_{(3, 40)} = 1.189$ ,  $p = 0.33$ . (Continued)

**FIGURE 4** | (\*\*); serum starvation effect:  $F_{(1, 40)} = 17.01, p < 0.001$  (\*\*\*) ; serum starvation  $\times$  gRNA interaction:  $F_{(3, 40)} = 1.818, p = 0.16$ . *Itgb6*: gRNA effect:  $F_{(3, 40)} = 0.4382, p = 0.7269$ ; serum starvation effect:  $F_{(1, 40)} = 1.075, p = 0.3060$ ; serum starvation  $\times$  gRNA interaction:  $F_{(3, 40)} = 0.4069, p = 0.7488$ . *Itgb8*: gRNA effect:  $F_{(3, 40)} = 0.9408, p = 0.4300$ ; serum starvation effect:  $F_{(1, 40)} = 1.302, p = 0.2606$ ; serum starvation  $\times$  gRNA interaction:  $F_{(3, 40)} = 0.3236, p = 0.8082$ . **(B)** Quantification of *Itgav*, *Itgb3*, *Itgb1*, *Itgb5*, *Itgb6*, and *Itgb8* mRNA levels in primary cortical neurons at different developmental stages. mRNA expression was normalized to the values of samples at 1 day *in vitro* (DIV) within the same RT-qPCR plate. \* $p < 0.05$ , \*\* $p < 0.01$ , \*\*\* $p < 0.001$ , repeated-measures one-way ANOVA followed by Tukey's post-test ( $n = 6$  from 3 independent cultures). F ratio and  $p$  values for repeated measures one-way ANOVA statistics are as follows, *Itgav*:  $F_{(1.894, 9.469)} = 0.7837, p = 0.4777$ . *Itgb3*:  $F_{(2.643, 13.21)} = 14.31, p = 0.0003$  (\*\*\*) . *Itgb1*:  $F_{(1.363, 6.813)} = 4.258, p = 0.0723$ . *Itgb5*:  $F_{(1.935, 9.676)} = 4.698, p = 0.0384$  (\*). *Itgb6*:  $F_{(2.051, 10.25)} = 18.29, p = 0.0004$  (\*\*\*) . *Itgb8*:  $F_{(1.894, 9.471)} = 39.24, p < 0.0001$  (\*\*\*) .

bottom left panel). The transcripts for *Itgav* and *Itgb1* remained stable from 1 to 16 DIV, while those for *Itgb6* and *Itgb8* decreased progressively during the same time period (**Figure 4B**). These data suggest therefore that the expression of  $\alpha V$  integrins is dynamically regulated during neuronal differentiation.

## DISCUSSION

Our findings indicate that CRISPRa for  $\alpha V$  integrins promotes neuronal differentiation of neuroblastoma N2a cells, without the need for serum deprivation. Further, they strongly suggest a subunit-specific role of  $\alpha V$  integrins in controlling neurite outgrowth. By combining CRISPRa, RT-qPCR and morphological analyses, we show that  $\alpha V\beta 3$  integrin initiates neuronal differentiation of N2a cells under proliferative conditions, while  $\alpha V\beta 5$  integrin is likely responsible for stabilizing neurites in cells already committed to differentiation.

Neuronal differentiation requires a series of consecutive steps starting with neural induction and cell proliferation events, followed by neuronal migration, neurite extension and axon-dendrite polarization. This precise differentiation program is due also to a coordinated rearrangement of the cytoskeleton in response to extracellular cues. Several integrins have been implicated in transducing extracellular signals to support outgrowth, branching or stabilization of neurites. For example, the laminin receptor  $\alpha 3\beta 1$  integrin signals through Arg kinase and p190RhoGAP to attenuate RhoA activity, thus stabilizing the dendritic arbor of adult, but not juvenile, hippocampal CA1 pyramidal neurons (Warren et al., 2012; Kerrisk et al., 2013), whereas  $\beta 3$  integrin contributes to establish a caudomedial-to-rostral lateral complexity gradient of basal dendrites in layer II/III cortical pyramidal neurons (Swinehart et al., 2020).

Integrins are also important for axon outgrowth. In the peripheral nervous system,  $\alpha 9\beta 1$  integrin functions as a receptor for the extracellular matrix protein tenascin-C, which is upregulated after injury, and indeed, exogenous expression of integrin  $\alpha 9$  in dorsal root ganglia neurons promotes some axonal regeneration into the dorsal root entry after dorsal column crush lesion, resulting in limited sensory recovery (Andrews et al., 2009).

Comparatively less is known about how  $\alpha V$  integrins, which are highly expressed in both neural progenitor cells and neurons (Pinkstaff et al., 1999; Hall et al., 2006), contribute to neurite outgrowth at early stages of differentiation. This group of integrins comprise five members (**Figure 1A**), whose expression is finely modulated during maturation of cortical neurons (**Figure 4B**).

To decipher their role in the initial steps of neurite outgrowth, we induced a 5 to 6-fold increase in the endogenous expression of  $\alpha V$  or  $\beta 3$  integrin subunits or both in N2a cells maintained in proliferative conditions. While both subunits promoted neuronal differentiation of N2a cells, we observed a stronger induction with  $\beta 3$  integrin. Given that this subunit pairs exclusively with the  $\alpha V$  in nucleated cells (Hynes, 2002; Lilja and Ivaska, 2018), an increase in  $\beta 3$  integrin expression levels is likely to shift the balance of all  $\alpha V$ -containing receptors towards the  $\alpha V\beta 3$  heterodimer. This  $\alpha V$  integrin appears therefore the most effective in promoting extension and branching of neurites in the initial phases of N2a cell differentiation.

The situation was surprisingly reversed in N2a cells already committed to neuronal differentiation by serum deprivation: neurite complexity was supported more effectively by activation of the  $\alpha V$  rather than the  $\beta 3$  subunit. Because boosting  $\alpha V$  expression in differentiated cells induced also a concomitant upregulation of the  $\beta 5$  subunit, we concluded that the  $\alpha V\beta 5$  heterodimer is likely the most important  $\alpha V$  integrin in stabilizing neurites at later stages of differentiation.

This shift in dependency for neurite arborization from  $\alpha V\beta 3$  to  $\alpha V\beta 5$  integrin likely reflects differences in subcellular localization or signalling between the two integrins (Baschieri et al., 2018; Lock et al., 2018; Zuidema et al., 2018), rather than a limited access to extracellular ligands. Indeed, both  $\alpha V\beta 3$  and  $\alpha V\beta 5$  integrins exhibit robust cell surface expression without the need for specific extracellular ligands (Sun et al., 2021), and the differences in neurite differentiation between the two heterodimers were observed irrespective of the plating substrate. The most prominent effect of fibronectin was actually to inhibit neurite outgrowth following CRISPRa for *Itgav* under proliferative conditions; in comparison, there were only minor effects of fibronectin upon CRISPRa for *Itgb3* or *Itgb3* and *Itgav* under the same proliferative conditions (compare **Figure 2C** with **Supplementary Figure S1C**).

Recent data show that  $\alpha V\beta 3$  integrin is able to bind fibronectin only in an extended-open conformation following high mechanical load (Bachmann et al., 2020; Jaudon et al., 2021), which may favour dynamic binding-unbinding to and from the substrate during early neuritogenesis. Indeed, in many cell types,  $\alpha V\beta 3$  integrin localizes in highly dynamic focal adhesion complexes linked to talin and actin stress fibers, while  $\alpha V\beta 5$  integrin has recently been found enriched in a new type of adhesion complex (referred to as flat clathrin lattices), which lacks classical adhesion proteins and associates with branched cortical actin, rather than actin stress fibers (Lock et al., 2018; Zuidema et al., 2018). Despite being rich in components of the clathrin-mediated endocytosis machinery, flat clathrin lattices are

highly static structures with very low endocytic activity. This is mainly due to  $\alpha V\beta 5$  integrin binding tightly to the substrate, thus preventing the formation of clathrin-coated pits (Bascieri et al., 2018). These unique features of  $\alpha V\beta 5$  integrin are most likely due to an insert of eight amino acids in the cytosolic tail of the  $\beta 5$  subunit, which is not found in any other beta subunit and may be responsible for the subcellular localization of  $\alpha V\beta 5$  integrin in flat clathrin lattices (Zuidema et al., 2018). Although these adhesion complexes have not been described in N2a cells and neurons, it is possible that  $\alpha V\beta 5$  integrin supports more static cell-substrate interactions that slow down outgrowth of neurites at early stages of neuronal differentiation, while effectively stabilizing them once formed.

Our results on the cooperation between  $\alpha V$  integrin heterodimers in regulating different stages of N2a cell differentiation are in line with previous findings in granule cell precursors of the developing cerebellum. In these cells,  $\alpha V\beta 3$  integrin contributes to suppressing proliferation, whereas  $\alpha V\beta 5$  integrin promotes the transition to granule cells and induces axon specification *via* a signalling pathway involving the kinases PI3K, Akt and GSK3 $\beta$  (Abe et al., 2018; Oishi et al., 2021). Therefore, a shift from  $\alpha V\beta 3$  integrin- to  $\alpha V\beta 5$  integrin-mediated cell adhesion might represent a general mechanism during development for promoting the transition from proliferating precursors to differentiating cells.

Here, we showed that CRISPRa can be used to regulate effectively the expression of these integrins, thereby promoting a coordinated progression of N2a cells towards a neuron-like phenotype. CRISPRa is not as prone as CRISPR-mediated genome editing to off-target effects because it does not rely on genomic DNA cleavage but requires persistent binding to a promoter region. Furthermore, the possibility of targeting one or multiple genes, using one or multiple gRNAs for each gene, and the availability of various transcriptional activators, such as VP64, VPR, SAM, and Suntag (Chavez et al., 2015; Konermann et al., 2015), as well as transcriptional repressors for CRISPR interference (CRISPRi), makes this system easily customizable to regulate precisely gene expression (Zheng et al., 2018; Zhou et al., 2018; Matharu et al., 2019; Savell et al., 2019). By contrast, overexpression paradigms are far less versatile and elevate the expression of the gene of interest by several folds with possible toxic effects (Jaudon et al., 2019). A temporally controlled activation of gene expression could be achieved by combining CRISPRa with inducible systems such as the tetracycline-dependent promoter (Tet) system (Dow et al., 2015; de Solis et al., 2016) or photoactivable proteins (Kawano et al., 2015). Thus,

it could be possible to switch the expression of distinct integrin subunits at specific steps of neuronal differentiation.

In summary, our findings show that CRISPRa-mediated enhancement of  $\alpha V$  integrins is a powerful and versatile strategy to induce neurite outgrowth and stabilization. These new tools could be used to promote neuronal differentiation of induced pluripotent stem cells, which express  $\alpha V$  integrins (Rowland et al., 2010), or to ameliorate neurite abnormalities in mouse models of brain disorders.

## DATA AVAILABILITY STATEMENT

The original contributions presented in the study are included in the article/**Supplementary Material**, further inquiries can be directed to the corresponding authors.

## AUTHOR CONTRIBUTIONS

SR performed cell culture and immunofluorescence experiments, imaging and morphological analyses, and contributed to writing the manuscript. FJ designed the gRNA constructs, performed molecular cloning, RT-qPCR experiments and Sholl analysis, and wrote the manuscript. LC supervised the project, wrote the manuscript and provided funding. All authors have approved the final version of the manuscript.

## FUNDING

Funding was provided by Compagnia San Paolo (Proposal ID: 2015 0702 to LC) and Fondazione Cariplo (Proposal ID: 2019-3438 to LC).

## ACKNOWLEDGMENTS

We thank members of the Cingolani Lab and A. Thalhammer for helpful discussions and critical reading of the manuscript.

## SUPPLEMENTARY MATERIAL

The Supplementary Material for this article can be found online at: <https://www.frontiersin.org/articles/10.3389/fgeed.2022.846669/full#supplementary-material>

## REFERENCES

- Abe, A., Hashimoto, K., Akiyama, A., Iida, M., Ikeda, N., Hamano, A., et al. (2018).  $\alpha V\beta 5$  Integrin Mediates the Effect of Vitronectin on the Initial Stage of Differentiation in Mouse Cerebellar Granule Cell Precursors. *Brain Res.* 1691, 94–104. doi:10.1016/j.brainres.2018.04.025
- Andrews, M. R., Czvitkovich, S., Dassie, E., Vogelaar, C. F., Faissner, A., Blits, B., et al. (2009).  $\alpha V\beta 5$  Integrin Promotes Neurite Outgrowth on Tenascin-C and Enhances Sensory Axon Regeneration. *J. Neurosci.* 29, 5546–5557. doi:10.1523/jneurosci.0759-09.2009
- Bachmann, M., Schäfer, M., Mykuliak, V. V., Ripamonti, M., Heiser, L., Weissenbruch, K., et al. (2020). Induction of Ligand Promiscuity of  $\alpha V\beta 3$  Integrin by Mechanical Force. *J. Cell Sci.* 133. doi:10.1242/jcs.242404
- Bachmann, M., Kukkurainen, S., Hytönen, V. P., and Wehrle-Haller, B. (2019). Cell Adhesion by Integrins. *Physiol. Rev.* 99, 1655–1699. doi:10.1152/physrev.00036.2018
- Bascieri, F., Dayot, S., Elkhatib, N., Ly, N., Capmany, A., Schauer, K., et al. (2018). Frustrated Endocytosis Controls Contractility-independent

- Mechanotransduction at Clathrin-Coated Structures. *Nat. Commun.* 9, 3825. doi:10.1038/s41467-018-06367-y
- Chavez, A., Scheiman, J., Vora, S., Pruitt, B. W., Tuttle, M., P R Iyer, E., et al. (2015). Highly Efficient Cas9-Mediated Transcriptional Programming. *Nat. Methods* 12, 326–328. doi:10.1038/nmeth.3312
- Cheyuo, C., Aziz, M., and Wang, P. (2019). Neurogenesis in Neurodegenerative Diseases: Role of MFG-E8. *Front. Neurosci.* 13, 569. doi:10.3389/fnins.2019.00569
- Chighizola, M., Dini, T., Lenardi, C., Milani, P., Podestà, A., and Schulte, C. (2019). Mechanotransduction in Neuronal Cell Development and Functioning. *Biophys. Rev.* 11, 701–720. doi:10.1007/s12551-019-00587-2
- Cingolani, L. A., and Goda, Y. (2008). Differential Involvement of  $\beta 3$  Integrin in Pre- and Postsynaptic Forms of Adaptation to Chronic Activity Deprivation. *Neuron Glia Biol.* 4, 179–187. doi:10.1017/s1740925x0999024x
- Cingolani, L. A., Thalhammer, A., Yu, L. M. Y., Catalano, M., Ramos, T., Colicos, M. A., et al. (2008). Activity-Dependent Regulation of Synaptic AMPA Receptor Composition and Abundance by  $\beta 3$  Integrins. *Neuron* 58, 749–762. doi:10.1016/j.neuron.2008.04.011
- de Solis, C. A., Ho, A., Holehonnur, R., and Ploski, J. E. (2016). The Development of a Viral Mediated CRISPR/Cas9 System with Doxycycline Dependent gRNA Expression for Inducible *In Vitro* and *In Vivo* Genome Editing. *Front. Mol. Neurosci.* 9, 70. doi:10.3389/fnmol.2016.00070
- Denoth-Lippuner, A., and Jessberger, S. (2021). Formation and Integration of New Neurons in the Adult hippocampus. *Nat. Rev. Neurosci.* 22, 223–236. doi:10.1038/s41583-021-00433-z
- Dow, L. E., Fisher, J., O'Rourke, K. P., Muley, A., Kasthuber, E. R., Livshits, G., et al. (2015). Inducible *In Vivo* Genome Editing with CRISPR-Cas9. *Nat. Biotechnol.* 33, 390–394. doi:10.1038/nbt.3155
- Fietz, S. A., Kelava, I., Vogt, J., Wilsch-Bräuninger, M., Stenzel, D., Fish, J. L., et al. (2010). OSVZ Progenitors of Human and Ferret Neocortex Are Epithelial-like and Expand by Integrin Signaling. *Nat. Neurosci.* 13, 690–699. doi:10.1038/nn.2553
- Gage, F. H., and Temple, S. (2013). Neural Stem Cells: Generating and Regenerating the Brain. *Neuron* 80, 588–601. doi:10.1016/j.neuron.2013.10.037
- Ghosh, H. S. (2019). Adult Neurogenesis and the Promise of Adult Neural Stem Cells. *J. Exp. Neurosci.* 13, 1179069519856876. doi:10.1177/1179069519856876
- Gilbert, L. A., Horlbeck, M. A., Adamson, B., Villalta, J. E., Chen, Y., Whitehead, E. H., et al. (2014). Genome-Scale CRISPR-Mediated Control of Gene Repression and Activation. *Cell* 159, 647–661. doi:10.1016/j.cell.2014.09.029
- Hall, P. E., Lathia, J. D., Miller, N. G. A., Caldwell, M. A., and Ffrench-Constant, C. (2006). Integrins Are Markers of Human Neural Stem Cells. *Stem Cells* 24, 2078–2084. doi:10.1634/stemcells.2005.0595
- Harrill, J. A., Chen, H., Streifel, K. M., Yang, D., Mundy, W. R., and Lein, P. J. (2015). Ontogeny of Biochemical, Morphological and Functional Parameters of Synaptogenesis in Primary Cultures of Rat Hippocampal and Cortical Neurons. *Mol. Brain* 8, 10. doi:10.1186/s13041-015-0099-9
- Hynes, R. O. (2002). Integrins. *Cell* 110, 673–687. doi:10.1016/s0092-8674(02)00971-6
- Jaudon, F., Thalhammer, A., and Cingolani, L. A. (2019). Correction of  $\beta 3$  Integrin Haplo-Insufficiency by CRISPRa Normalizes Cortical Network Activity. *BioRxiv* [Preprint]. doi:10.1101/664706
- Jaudon, F., Thalhammer, A., and Cingolani, L. A. (2021). Integrin Adhesion in Brain Assembly: From Molecular Structure to Neuropsychiatric Disorders. *Eur. J. Neurosci.* 53, 3831–3850. doi:10.1111/ejn.14859
- Johansson, S., Svineng, G., Wennerberg, K., Armulik, A., and Lohikangas, L. (1997). Fibronectin-integrin Interactions. *Front. Biosci.* 2, d126–146. doi:10.2741/a178
- Kawano, F., Suzuki, H., Furuya, A., and Sato, M. (2015). Engineered Pairs of Distinct Photoswitches for Optogenetic Control of Cellular Proteins. *Nat. Commun.* 6, 6256. doi:10.1038/ncomms7256
- Kerrisk, M. E., Cingolani, L. A., and Koleske, A. J. (2014). ECM Receptors in Neuronal Structure, Synaptic Plasticity, and Behavior. *Prog. Brain Res.* 214, 101–131. doi:10.1016/b978-0-444-63486-3.00005-0
- Kerrisk, M. E., Greer, C. A., and Koleske, A. J. (2013). Integrin 3 Is Required for Late Postnatal Stability of Dendrite Arbors, Dendritic Spines and Synapses, and Mouse Behavior. *J. Neurosci.* 33, 6742–6752. doi:10.1523/jneurosci.0528-13.2013
- Konermann, S., Brigham, M. D., Trevino, A. E., Joung, J., Abudayyeh, O. O., Barcena, C., et al. (2015). Genome-scale Transcriptional Activation by an Engineered CRISPR-Cas9 Complex. *Nature* 517, 583–588. doi:10.1038/nature14136
- Korotchenko, S., Cingolani, L. A., Kuznetsova, T., Bologna, L. L., Chiappalone, M., and Dityatev, A. (2014). Modulation of Network Activity and Induction of Homeostatic Synaptic Plasticity by Enzymatic Removal of Heparan Sulfates. *Phil. Trans. R. Soc. B* 369, 20140134. doi:10.1098/rstb.2014.0134
- Lilja, J., and Ivaska, J. (2018). Integrin Activity in Neuronal Connectivity. *J. Cell Sci* 131. doi:10.1242/jcs.212803
- Lock, J. G., Jones, M. C., Askari, J. A., Gong, X., Oddone, A., Olofsson, H., et al. (2018). Reticular Adhesions Are a Distinct Class of Cell-Matrix Adhesions that Mediate Attachment during Mitosis. *Nat. Cell Biol* 20, 1290–1302. doi:10.1038/s41556-018-0220-2
- Matharu, N., Rattanasopha, S., Tamura, S., Maliskova, L., Wang, Y., Bernard, A., et al. (2019). CRISPR-mediated Activation of a Promoter or Enhancer Rescues Obesity Caused by Haploinsufficiency. *Science* 363. doi:10.1126/science.aau0629
- McGeachie, A. B., Cingolani, L. A., and Goda, Y. (2011). A Stabilising Influence: Integrins in Regulation of Synaptic Plasticity. *Neurosci. Res.* 70, 24–29. doi:10.1016/j.neures.2011.02.006
- McGeachie, A. B., Skrzypiec, A. E., Cingolani, L. A., Letellier, M., Pawlak, R., and Goda, Y. (2012).  $\beta 3$  Integrin Is Dispensable for Conditioned Fear and Hebbian Forms of Plasticity in the hippocampus. *Eur. J. Neurosci.* 36, 2461–2469. doi:10.1111/j.1460-9568.2012.08163.x
- Oishi, Y., Hashimoto, K., Abe, A., Kuroda, M., Fujii, A., and Miyamoto, Y. (2021). Vitronectin Regulates the Axon Specification of Mouse Cerebellar Granule Cell Precursors via  $\alpha v\beta 5$  Integrin in the Differentiation Stage. *Neurosci. Lett.* 746, 135648. doi:10.1016/j.neulet.2021.135648
- Park, Y. K., and Goda, Y. (2016). Integrins in Synapse Regulation. *Nat. Rev. Neurosci.* 17, 745–756. doi:10.1038/nrn.2016.138
- Perez-Pinera, P., Kocak, D. D., Vockley, C. M., Adler, A. F., Kabadi, A. M., Polstein, L. R., et al. (2013). RNA-guided Gene Activation by CRISPR-Cas9-Based Transcription Factors. *Nat. Methods* 10, 973–976. doi:10.1038/nmeth.2600
- Pinkstaff, J. K., Detterich, J., Lynch, G., and Gall, C. (1999). Integrin Subunit Gene Expression Is Regionally Differentiated in Adult Brain. *J. Neurosci.* 19, 1541–1556. doi:10.1523/jneurosci.19-05-01541.1999
- Prowse, A. B. J., Chong, F., Gray, P. P., and Munro, T. P. (2011). Stem Cell Integrins: Implications for *Ex-Vivo* Culture and Cellular Therapies. *Stem Cell Res.* 6, 1–12. doi:10.1016/j.scr.2010.09.005
- Ran, F. A., Hsu, P. D., Wright, J., Agarwala, V., Scott, D. A., and Zhang, F. (2013). Genome Engineering Using the CRISPR-Cas9 System. *Nat. Protoc.* 8, 2281–2308. doi:10.1038/nprot.2013.143
- Rowland, T. J., Miller, L. M., Blaschke, A. J., Doss, E. L., Bonham, A. J., Hikita, S. T., et al. (2010). Roles of Integrins in Human Induced Pluripotent Stem Cell Growth on Matrigel and Vitronectin. *Stem Cell Dev.* 19, 1231–1240. doi:10.1089/scd.2009.0328
- Savell, K. E., Bach, S. V., Zipperly, M. E., Revanna, J. S., Goska, N. A., Tuscher, J. J., et al. (2019). A Neuron-Optimized CRISPR/dCas9 Activation System for Robust and Specific Gene Regulation. *eNeuro* 6. doi:10.1523/ENEURO.0495-18.2019
- Schmid, R. S., and Anton, E. S. (2003). Role of Integrins in the Development of the Cerebral Cortex. *Cereb. Cortex* 13, 219–224. doi:10.1093/cercor/13.3.219
- Schubert, D., Humphreys, S., Baroni, C., and Cohn, M. (1969). *In Vitro* Differentiation of a Mouse Neuroblastoma. *Proc. Natl. Acad. Sci. U.S.A.* 64, 316–323. doi:10.1073/pnas.64.1.316
- Stenzel, D., Wilsch-Bräuninger, M., Wong, F. K., Heuer, H., and Huttner, W. B. (2014). Integrin  $\alpha v\beta 3$  and Thyroid Hormones Promote Expansion of Progenitors in Embryonic Neocortex. *Development* 141, 795–806. doi:10.1242/dev.101907
- Sun, G., Guillon, E., and Holley, S. A. (2021). Integrin Intra-heterodimer Affinity Inversely Correlates with Integrin Activatability. *Cell Rep.* 35, 109230. doi:10.1016/j.celrep.2021.109230
- Swinehart, B. D., Bland, K. M., Holley, Z. L., Lopuch, A. J., Casey, Z. O., Handwerk, C. J., et al. (2020). Integrin  $\beta 3$  Organizes Dendritic Complexity of Cerebral Cortical Pyramidal Neurons along a Tangential Gradient. *Mol. Brain* 13, 168. doi:10.1186/s13041-020-00707-0
- Takada, Y., Ye, X., and Simon, S. (2007). The Integrins. *Genome Biol.* 8, 215. doi:10.1186/gb-2007-8-5-215
- Thalhammer, A., and Cingolani, L. A. (2014). Cell Adhesion and Homeostatic Synaptic Plasticity. *Neuropharmacology* 78, 23–30. doi:10.1016/j.neuropharm.2013.03.015

- Thalhammer, A., Contestabile, A., Ermolyuk, Y. S., Ng, T., Volynski, K. E., Soong, T. W., et al. (2017). Alternative Splicing of P/Q-Type Ca<sup>2+</sup> Channels Shapes Presynaptic Plasticity. *Cell Rep.* 20, 333–343. doi:10.1016/j.celrep.2017.06.055
- Thalhammer, A., Jaudon, F., and Cingolani, L. A. (2018). Combining Optogenetics with Artificial microRNAs to Characterize the Effects of Gene Knockdown on Presynaptic Function within Intact Neuronal Circuits. *J. Vis. Exp.* 133, 57223. doi:10.3791/57223
- Vandesompele, J., De Preter, K., Pattyn, F., Poppe, B., Van Roy, N., De Paepe, A., et al. (2002). Accurate Normalization of Real-Time Quantitative RT-PCR Data by Geometric Averaging of Multiple Internal Control Genes. *Genome Biol.* 3, RESEARCH0034. doi:10.1186/gb-2002-3-7-research0034
- Wang, A. G., Yen, M. Y., Hsu, W. M., and Fann, M. J. (2006). Induction of Vitronectin and Integrin Alpha<sub>v</sub> in the Retina after Optic Nerve Injury. *Mol. Vis.* 12, 76–84.
- Warren, M. S., Bradley, W. D., Gourley, S. L., Lin, Y.-C., Simpson, M. A., Reichardt, L. F., et al. (2012). Integrin 1 Signals through Arg to Regulate Postnatal Dendritic Arborization, Synapse Density, and Behavior. *J. Neurosci.* 32, 2824–2834. doi:10.1523/jneurosci.3942-11.2012
- Wojcik-Stanaszek, L., Gregor, A., and Zalewska, T. (2011). Regulation of Neurogenesis by Extracellular Matrix and Integrins. *Acta Neurobiol. Exp. (Wars)* 71, 103–112.
- Zheng, Y., Shen, W., Zhang, J., Yang, B., Liu, Y.-N., Qi, H., et al. (2018). CRISPR Interference-Based Specific and Efficient Gene Inactivation in the Brain. *Nat. Neurosci.* 21, 447–454. doi:10.1038/s41593-018-0077-5
- Zhou, H., Liu, J., Zhou, C., Gao, N., Rao, Z., Li, H., et al. (2018). *In Vivo* simultaneous Transcriptional Activation of Multiple Genes in the Brain Using CRISPR-dCas9-Activator Transgenic Mice. *Nat. Neurosci.* 21, 440–446. doi:10.1038/s41593-017-0060-6
- Zuidema, A., Wang, W., Kreft, M., Te Molder, L., Hoekman, L., Bleijerveld, O. B., et al. (2018). Mechanisms of Integrin  $\alpha$ V $\beta$ 5 Clustering in Flat Clathrin Lattices. *J. Cell Sci.* 131. doi:10.1242/jcs.221317

**Conflict of Interest:** The authors declare that the research was conducted in the absence of any commercial or financial relationships that could be construed as a potential conflict of interest.

**Publisher's Note:** All claims expressed in this article are solely those of the authors and do not necessarily represent those of their affiliated organizations, or those of the publisher, the editors and the reviewers. Any product that may be evaluated in this article, or claim that may be made by its manufacturer, is not guaranteed or endorsed by the publisher.

Copyright © 2022 Riccardi, Cingolani and Jaudon. This is an open-access article distributed under the terms of the Creative Commons Attribution License (CC BY). The use, distribution or reproduction in other forums is permitted, provided the original author(s) and the copyright owner(s) are credited and that the original publication in this journal is cited, in accordance with accepted academic practice. No use, distribution or reproduction is permitted which does not comply with these terms.

*Supplementary Material*

**CRISPR-mediated activation of  $\alpha V$  integrin subtypes promotes neuronal differentiation of neuroblastoma Neuro2a cells**

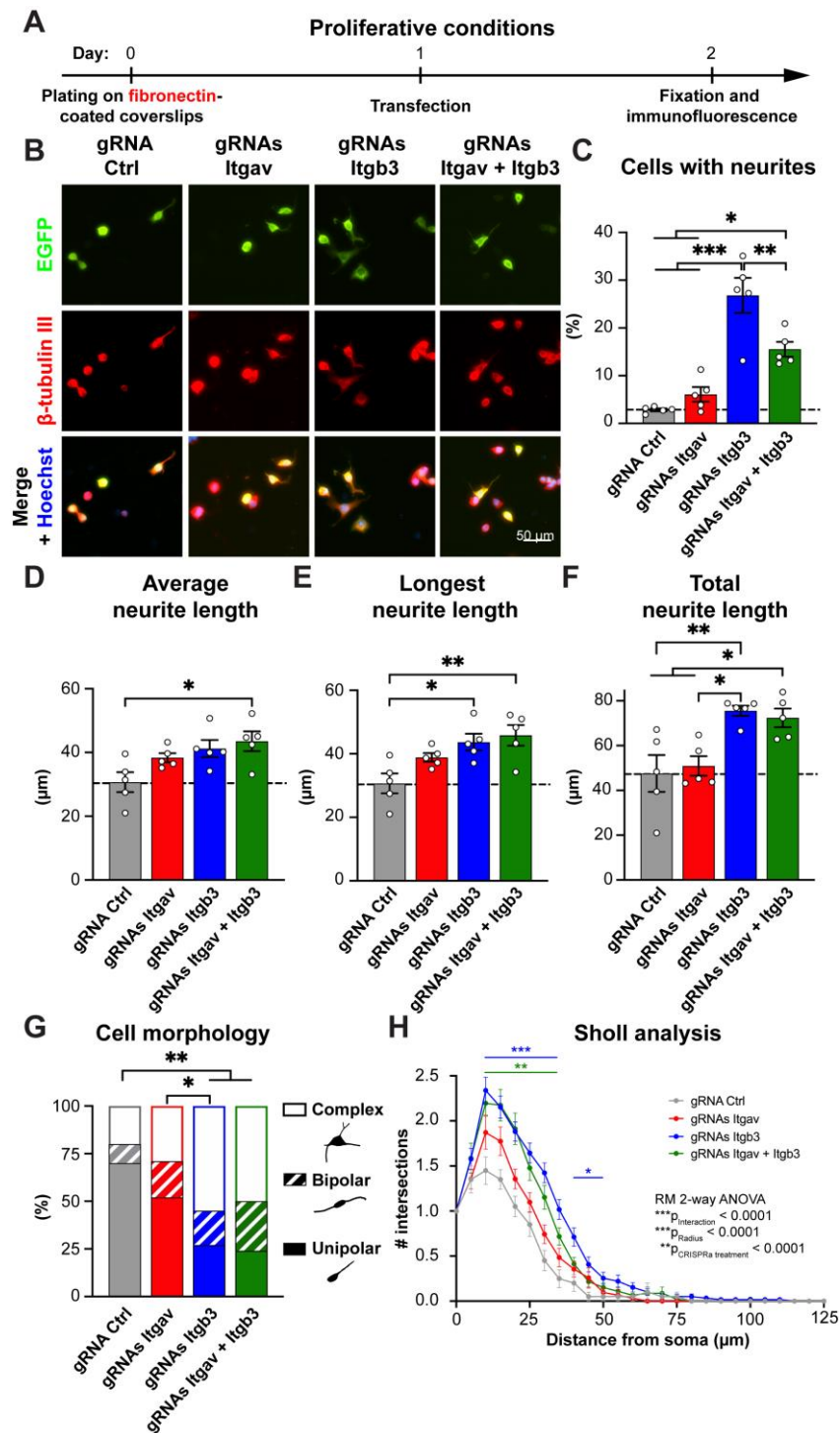
**Sara Riccardi<sup>1,2</sup>, Lorenzo A. Cingolani<sup>1,3</sup> and Fanny Jaudon<sup>1,4</sup>**

<sup>1</sup>Department of Life Sciences, University of Trieste, Trieste, Italy

<sup>2</sup>Department of Experimental Medicine, University of Genoa, Genoa, Italy

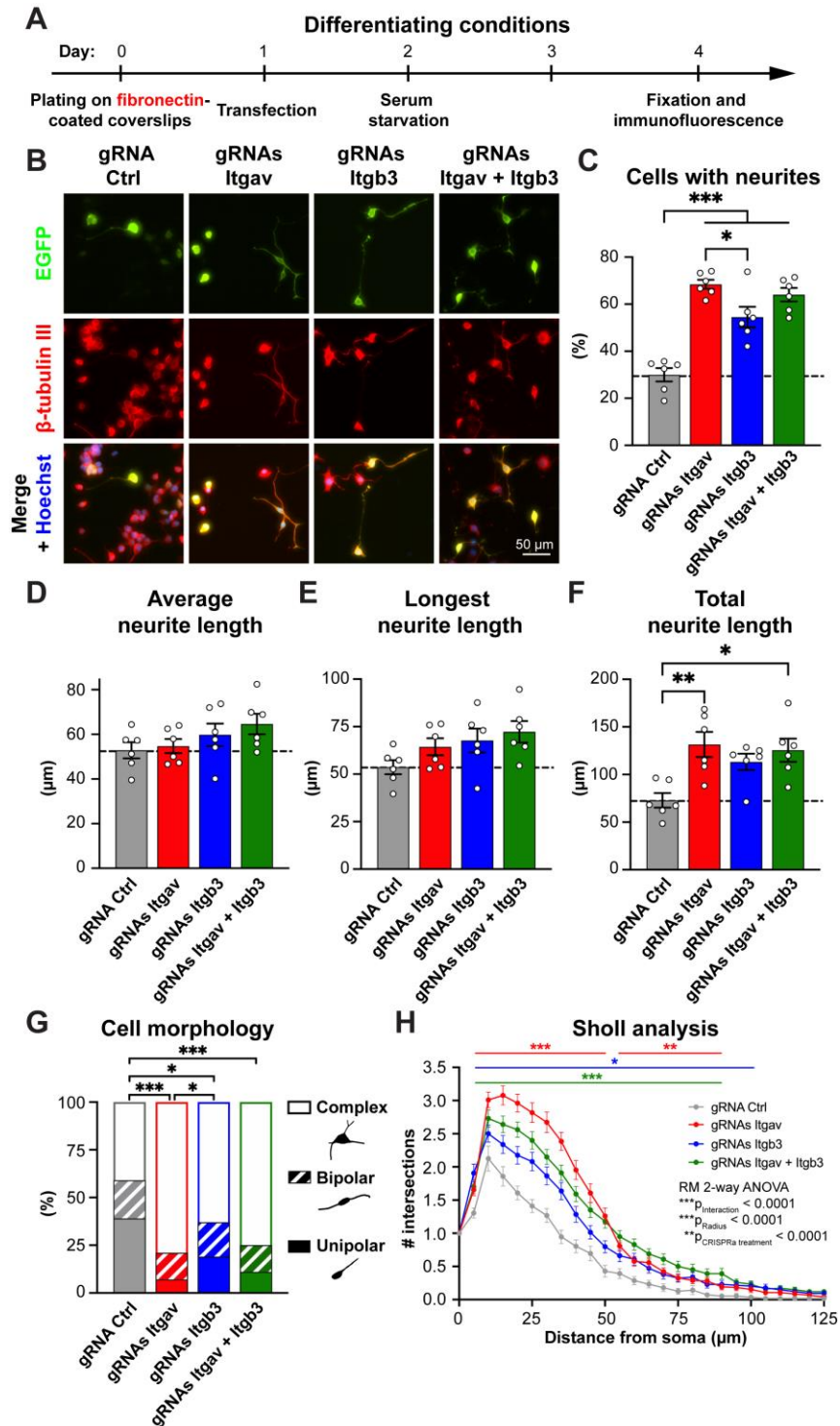
<sup>3</sup>Center for Synaptic Neuroscience and Technology (NSYN), Istituto Italiano di Tecnologia (IIT), Genoa, Italy

<sup>4</sup>IRCCS Ospedale Policlinico San Martino, Genoa, Italy



**Supplementary Figure 1. Differentiation of N2a cells plated on fibronectin under proliferative conditions upon CRISPRa for *Ilgav* and/or *Irgb3*.** (A) Time course of the experiment. (B) Representative images of N2a cells expressing the indicated constructs. Transfection was verified by EGFP expression, β-tubulin III staining was used to trace neurites and Hoechst to stain nuclei. (C) Percentage of cells with neurites within EGFP-positive cells for experiments as in (A, B). \* $p < 0.05$ , \*\* $p < 0.01$ , \*\*\* $p < 0.001$  one-way ANOVA followed by Tukey's post-test ( $n = 5$  coverslips from 3

independent experiments). CRISPRa for *Itgb3* induces differentiation of N2a cells. **(D-F)** Average (D), longest (E) and total neurite length (F) of differentiated N2a cells expressing the indicated constructs. \* $p < 0.05$ , \*\* $p < 0.01$ , one-way ANOVA followed by Tukey's post-test (n=5 coverslips from 3 independent cultures). **(G)** Morphological classification of differentiated N2a cells. \* $p < 0.05$ , \*\* $p < 0.01$ , Chi-square test (n=20, 31, 59 and 46 cells from 3 independent experiments for gRNA Ctrl, gRNAs *Itgav*, gRNAs *Itgb3* and gRNAs *Itgav + Itgb3*, respectively). **(H)** Sholl analysis of differentiated N2a cells. \* $p < 0.05$ , \*\* $p < 0.01$ , \*\*\* $p < 0.001$  relative to gRNA Ctrl, repeated measures ANOVA followed by Dunnett's post-test (n=20, 31, 59 and 46 cells from 3 independent experiments for gRNA Ctrl, gRNAs *Itgav*, gRNAs *Itgb3* and gRNAs *Itgav + Itgb3*, respectively). CRISPRa for *Itgb3* induces a complex arborization.



**Supplementary Figure 2. Differentiation of N2a cells plated on fibronectin under differentiating conditions upon CRISPRa for *Itgav* and/or *Itgb3*.** (A) Time course of the experiment. (B) Representative images of N2a cells expressing the indicated constructs. Transfection was verified by EGFP expression, β-tubulin III staining was used to trace neurites and Hoechst to stain nuclei. (C) Percentage of cells with neurites within EGFP-positive cells for experiments as in (A, B). \* $p < 0.05$ , \*\*\* $p < 0.001$ , one-way ANOVA followed by Tukey's post-test ( $n = 6$  coverslips from 3 independent

experiments). CRISPRa for either *Itgav* or *Itgb3* or both doubles the percentage of differentiated N2a cells, as compared to control conditions. **(D-F)** Average (C), longest (D) and total neurite length (E) of differentiated N2a cells expressing the indicated constructs. \* $p < 0.05$ , \*\* $p < 0.01$ , one-way ANOVA followed by Tukey's post-test (n=6 coverslips from 3 independent experiments). **(G)** Morphological classification of differentiated N2a cells. \* $p < 0.05$ , \*\*\* $p < 0.001$ , Chi-square test (n=56, 104, 74 and 100 cells from 3 independent experiments for gRNA Ctrl, gRNAs *Itgav*, gRNAs *Itgb3* and gRNAs *Itgav* + *Itgb3*, respectively). **(H)** Sholl analysis of differentiated N2a cells. \* $p < 0.05$ , \*\* $p < 0.01$ , \*\*\* $p < 0.001$  relative to gRNA Ctrl, repeated measures ANOVA followed by Dunnett's post-test (n=56, 104, 74 and 100 cells from 3 independent experiments for gRNA Ctrl, gRNAs *Itgav*, gRNAs *Itgb3* and gRNAs *Itgav* + *Itgb3*, respectively). CRISPRa for *Itgav* induces a complex arborization.

**Supplementary Table 1. List of RT-qPCR primers used.**

<b>Gene</b>	<b>GenBank Accession</b>	<b>Forward sequence (5' → 3')</b>	<b>Reverse sequence (5' → 3')</b>
Itgav	NM_008402.3	ATTGACGGGCCAATGAACTG	ATTCCACAGCCCAAAGTGTG
Itgb1	NM_010578.2	CTTATTGGCCTTGCCTTGCT	GATTTTCACCCGTGTCCCAC
Itgb3	NM_016780.2	GGGCGTTGTTGTTGGAGAG	ACAAAGTCTCATCTGAGCACCAG
Itgb5	NM_001145884.1	CCGTGAGCCGGAGCG	GCATATGTTGAGCCCTGCG
Itgb6	NM_001159564.1	ATCATGTTGGGGGTGTCACT	ACAGAGGATTGGTTCCCGTT
Itgb8	NM_177290.3	CTGCCGTCTGTGAGAGTCAT	CGTCATTTCGGCACCCTATG
Actb	NM_007393.5	TTGCTGACAGGATGCAGAAG	AGTCCGCCTAGAAGCACTTG
Gapdh	NM_001289726.1	TGTGTCCGTCGTGGATCTGA	CCTGCTTACCACCTTCTTGA
Hprt1	NM_013556.2	AAGCTTGCTGGTGAAAAGGA	TTGCGCTCATCTTAGGCTTT